Mechanisms of Development 158 (2019) 103555

Contents lists available at ScienceDirect

Mechanisms of Development

journal homepage: www.elsevier.com/locate/mod

The *microRNA*-306/*abrupt* regulatory axis controls wing and haltere growth in *Drosophila*

Carolina J. Simoes da Silva[a], Ismael Sospedra[a], Ricardo Aparicio[b], Ana Busturia[a,*]

[a] Centro de Biología Molecular "Severo Ochoa", CSIC-UAM, Nicolás Cabrera 1, 28049 Madrid, Spain
[b] Department of Integrative Biology and Physiology, University of California, Los Angeles, CA 90095, USA

ARTICLE INFO

Keywords:
Abrupt
miR-306
Cyclin E
Dacapo
Growth
Haltere
Wing
Drosophila

ABSTRACT

Growth control relies on extrinsic and intrinsic mechanisms that regulate and coordinate the size and pattern of organisms. This control is crucial for a homeostatic development and healthy physiology. The gene networks acting in this process are large and complex: factors involved in growth control are also important in diverse biological processes and these networks include multiple regulators that interact and respond to intra- and extracellular inputs that may ultimately converge in the control of the cell cycle. In this work we have studied the function of the *Drosophila abrupt* gene, coding for a BTB-ZF protein and previously reported to be required for wing vein pattern, in the control of haltere and wing growth. We have found that inactivation of *abrupt* reduces the size of the wing and haltere. We also found that the microRNA *miR-306* controls *abrupt* expression and that *miR-306* and *abrupt* genetically interact to control wing size. Moreover, the reduced appendage size due to *abrupt* inactivation is rescued by overexpression of *Cyclin-E* and by inactivation of *dacapo*. These findings define a *miR-306-abrupt* regulatory axis that controls wing and haltere size, whereby *miR-306* maintains appropriate levels of *abrupt* expression which, in turn, regulates the cell cycle. Thus, our results uncover a novel function of *abrupt* in the regulation of the size of *Drosophila* appendages during development and contribute to the understanding of the coordination between growth and pattern as well as to the understanding of *abrupt* oncogenic function in flies.

1. Introduction

The organized actions of cellular processes such as growth, cell division, proliferation, apoptosis and differentiation are required to achieve the appropriate size and shape of the tissues and organs that constitute the organism (Lander, 2011; Lewis, 2008). Multiple signaling pathways are currently known to direct all these processes and the interplay of intrinsic factors, such as transcription factors and microRNAs, as well as extrinsic factors, such as hormones, define the final size of an organ (Day and Lawrence, 2000; Johnston and Gallant, 2002; Neto-Silva et al., 2009; Pan, 2010). Yet the challenge remains to describe the complete molecular regulatory network that eventually initiates a particular cellular response to ensure the appropriate size that permits healthy development and physiological fitness.

Drosophila has served as an excellent model to study growth and pattern regulation (Mirth and Shingleton, 2012; Vollmer et al., 2017). In particular, the proliferating larval epithelial groups of cells, known as imaginal discs, that form the fly adult appendages such as the wing and haltere, have been extensively studied (Beira and Paro, 2016). The wing and haltere imaginal discs are different in shape and size but follow the same developmental program mediated by nearly the same molecular pathways, including the *Decapentaplegic* signaling pathway (Restrepo et al., 2014; Teleman and Cohen, 2000). Differences in size and pattern between wing and haltere are controlled by the homeotic *Ultrabithorax* (*Ubx*) gene (Smolik-Utlaut, 1990; de Navas et al., 2006; Roch and Akam, 2000). *Ubx* is specifically expressed in the haltere disc and differentially regulates downstream effectors of common regulatory pathways to repress haltere growth and to avoid developing wing morphological features such as the appearance of wing veins (named L1–L5) and wing margin bristles (Weatherbee et al., 1998). Genes controlling growth have been many times described to both have an influence on and be influenced by patterning (Day and Lawrence, 2000). However, the understanding of the coordination of growth and pattern control is far from complete. Further analysis of the genes and mechanisms required for patterning control should lead to a more complete understanding of growth control. Both transcription factors and microRNAs play important functions in growth regulatory networks and are capable of regulating gene expression of many genes

* Corresponding author.
E-mail address: abusturia@cbm.csic.es (A. Busturia).

https://doi.org/10.1016/j.mod.2019.103555
Received 19 December 2018; Received in revised form 6 May 2019; Accepted 14 May 2019
Available online 18 May 2019
0925-4773/ © 2019 Elsevier B.V. All rights reserved.

(Hammonds et al., 2013). In this work, we have analyzed the function of the *abrupt* gene in wing and haltere growth control and its regulation mediated by microRNAs.

The *abrupt* gene, encoding a BTB-ZF finger regulatory protein, was originally reported to be required for the patterning of the L5 vein of the wing and motoneuron morphogenesis (Cook et al., 2004; Hu et al., 1995). Later studies have shown that *abrupt* is involved in a diversity of functions during development such as neurogenesis (Hattori et al., 2013; Li et al., 2004; Sugimura et al., 2004) and border cell migration (Jang et al., 2009). More recently, *abrupt* has been reported to function as an epithelia oncogene (Turkel et al., 2013), suggesting a role in growth control. High levels of Abrupt in the eye imaginal discs induce hyperplasic over-proliferation that can be transformed to neoplasic proliferation when, in addition to high levels of Abrupt, the function of the *scribble* gene is inactivated (Turkel et al., 2013). Moreover, high levels of Abrupt in the wing imaginal discs also induce over-proliferation (Simoes da Silva et al., 2017), further suggesting a role of abrupt in wing growth control.

How the levels of *abrupt* are maintained and how *abrupt* controls growth is poorly understood. MicroRNAs are good candidates to participate in networks controlling expression levels of transcription factors. In *Drosophila*, there exist roughly 300 microRNAs, some of them shown to be involved in growth control (www.mirbase.org; Becam et al., 2011; Bejarano et al., 2012; Herranz et al., 2010; Waldron and Newbury, 2012). Previous work has identified binding sites for the microRNA *miR-306* in the 3′-UTR of the *abrupt* gene (Bejarano et al., 2012), suggesting that *miR-306* could be involved in the maintenance of *abrupt* levels. The microRNA *miR-306* is conserved across the Drosophilids and other insects (www.mirbase.org, Ge et al., 2013; Jagadeeswaran et al., 2010; Macedo et al., 2016; Ylla et al., 2016) and is a member of the *miR-9c*, *miR-9b*, *miR-79* cluster (Chen et al., 2014). *miR-306* has been reported to be expressed in the wing imaginal disc (Herranz et al., 2010) and has been shown to participate in stem cell differentiation pathway by down-regulating *bag of marbles* expression thus allowing spermatid terminal differentiation (Eun et al., 2013). Moreover, ChIP-seq analysis as well as RNA-seq analysis have revealed that Abrupt could act as regulator of the cell cycle. Furthermore, it has been reported that *cdk2* mRNA expression is upregulated upon Abrupt overexpression and Abrupt protein has been found to be bound to *cdk2* regulatory sequences (Turkel et al., 2013). Thus, we hypothesize that *miR-306* is an upstream regulator of *abrupt* and, in turn, that Abrupt can control growth by controlling the cell cycle.

Here we show that inactivation of *abrupt* function produces a decrease in the size of both the haltere and wing of the fly and that the reduction of the wing size is related to the reduction of cell size. Further, we report that *miR-306* regulates *abrupt* expression and that *miR-306* genetically interacts with *abrupt* to regulate wing size. Based on these results, we propose a *miR-306/abrupt* regulatory axis that controls growth. Finally, we provide evidence supporting the function of *abrupt* in growth control through the regulation of the cell cycle.

2. Material and methods

2.1. Drosophila stocks and fly husbandry

The following stocks were used y^1w^{1118} (control), $Df(1)w^{67c23}$;*If/CyO;MKRS/TM6B*, ab^1 (Morgan et al., 1925), ab^{clu1}, $Df(1)w^{67c23}$;*P{EPgy2}* $ab^{EY01129}$ (Vactor et al., 1993), *miR-306-79-9b KO* (Chen et al., 2014), Ubx^{130}/*TM6B* (Kauffman, 1981), pbx^1/*TM6B*, bx^3/*TM6B* (Bender et al., 1983), *PBac [ab-GFP.FLAG]* (referred to in the text as *ab-GFP*, BDSC #38626), *3′UTR-ab-GFP* (Okamura et al., 2008), ptc^{PyR68} (referred to in the text as *ptc-DsRed*) (Akimoto et al., 2005), and hh^{PyR215} (referred to in the text as *hh-DsRed*) (Akimoto et al., 2005). For overexpression experiments the GAL4/UAS system (Brand and Perrimon, 1993) was used at 17 °C, 25 °C or 29 °C with the following GAL4 lines: *scalloped-Gal4* (*sdG4*) (Calleja, M and Morata, G., unpublished), *cubitus interruptus-Gal4* (*ciG4*), *patched-Gal4* (*ptcG4*), *apterous-Gal4* (*apG4*), *hedgehog-Gal4* (*hhG4*) and *daughterless-Gal4* (*daG4*) previously described in www.Flybase.org together with the following UAS lines: *UAS GFP-miR-306sp;UAS GFP-miR-306sp* (Eun et al., 2013), *UAS GFP-miR-306*^{xc}(Eun et al., 2013), *UAS miR-306*^{20}*-DsRed* (this work), *UAS* ab^{55}(Cook et al., 2004), *UAS CycE* (Richardson et al., 1995), *UAS Ubx* (Castelli-Gair et al., 1994), *UAS DIAP1* (Hay et al., 1995), *UAS DΔNp53* (Dichtel-Danjoy et al., 2013), *UAS GFP*, *UAS LacZ* (previously described in www.flybase.org), *UAS* dap_{RNAi} (TRiP line #HMS01610), *UAS* ab_{RNAi} (TRiP line #HMS00369), *UAS* ab_{RNAi} (TRiP.line #HMS29407) and *UAS* Ubx_{RNAi} (VDRC #37825) (Dietzl et al., 2007).

To control similar growth conditions for wing size measurements, crosses were established in the same size vials containing the same amount of standard fly food. Moreover, parental flies (usually about 2:1 females:males rate) were transferred to a new vial every 24 h and female progeny was selected for measurements. To select imaginal discs at the same developmental stage from late third-instar larvae (96-120 h old), the progeny of specific crosses were grown in food containing 5% Bromophenol blue (Sigma-Aldrich).

2.2. Generation of the UAS-miR-306-DsRed constructs and transgenic flies

A 356-bp fragment containing the *miR-306* genomic sequence was obtained by PCR amplification of *Drosophila* genomic DNA using the following primers 5′-CTGGACACCTTGGCTATTTCGC-3′ and 5′-GCTAA AGCGCCAAAGCAATGGC-3′ and cloned into pGEM-T easy vector (Promega) to generate the *pGEM-miR-306* plasmid. *pGEM-miR-306* was digested with *NotI* and the resulting fragment was cloned into *NotI*-digested *pUAST-DsRed* to obtain the *pUAST-miR-306-DsRed* construct. *pUAST-miR-306-DsRed* was sequenced to confirm the correct orientation and sequence of the microRNA. Transgenic flies were generated by standard methods using y^1w^{1118} as host flies at the Drosophila Transgenic Service (CBMSO, Madrid, Spain). Twelve independent lines were obtained, mapped (2 on the X, 6 on the II, and 4 on the III chr.) and the strength of the overexpression was characterized by analyzing the wing phenotypes of flies *sdG4;UAS miR-306* (lines 1–12) grown at 29 °C. The overexpression of *miR-306* using the lines 1–12 resulted in “strong”, “moderate” and “weak” wing phenotypes (both in size and morphology). A line with an insertion on the III chr with a “moderate” wing phenotype was used for this work.

2.3. Wing and leg size measurements, trichome quantification and statistical analysis

For wing size measurements, the wing contours were measured and processed using the Image J software. Photographs of the wings were taken using the same optical conditions in a Zeiss CCD or in a Leica DM5000 microscopes coupled to a color camera. For leg size measurements, the length of the female leg femur was analyzed following a similar method previously described (Grubbs et al., 2013), drawing a straight line (Supplementary Fig. 2) from the most distal constriction of the trochanter until the end of the femur segment. For quantification of trichomes per area, the number of trichomes was manually counted in the corresponding wing areas using Image J software.

Statistical analysis was performed using the unpaired *t*-test (when comparing two groups of data sets) or one-way ANOVA analysis with Tukey post-test (when comparing more than two groups of data sets) using the GraphPad Prism software. Data represent the mean + SEM (Standard Error of the Mean). Statistical significance is indicated with asterisks corresponding to the following p-values: $0.01 < p^* < 0.05$, $0.001 < p^{**} < 0.01$ and $^{***}p < 0.001$.

2.4. Immuno-staining, microscopy and fluorescence quantification

Imaginal discs from third instar larvae were dissected and stained as previously described (Simoes da Silva et al., 2017). The following

primary antibodies were used: rabbit anti-Abrupt (1:200) (kindly provided by S. Crews, Hu et al., 1995), rabbit anti-activated Caspase-3 (1:50) (Cell Technologies), mouse anti-Ultrabithorax (1:20) (Iowa Hybridoma Bank) and To-PRO3 (Invitrogen).

Secondary fluorescent antibodies were coupled to Rhodamin RedX and FYCT (1:500) (Jackson Immuno Research). Imaginal discs were mounted in Vectashield (Vector Laboratories) or DAKO medium (Dako Inc.). Images were generated using a LSM510 confocal microscope (Zeiss). Images were processed with Adobe Photoshop CS5. For 3rd instar wing and haltere disc size quantifications, the contour of *sdG4/+; UAS GFP/+* and the contour of the wing pouch were used to determine the corresponding areas. For the anterior (A) and posterior (P)

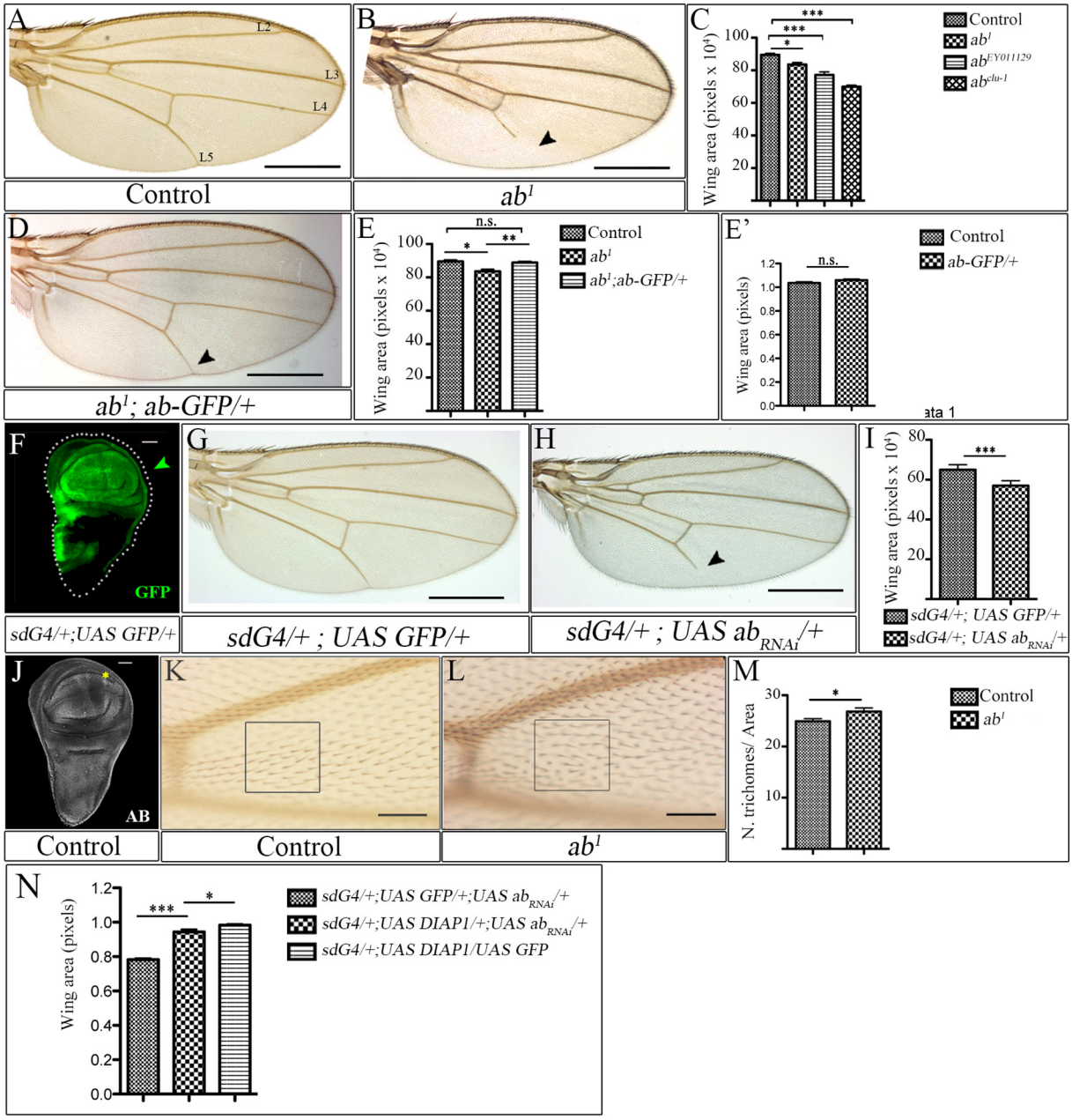

Fig. 1. Inactivation of *abrupt* function causes a reduction in wing size. A) Wing y^1w^{1118} (used as a control), the L2–L5 veins are indicated. B) Wing ab^1 homozygous. Note the reduction of wing size and the shortening of the L5 vein (arrowhead). C) Graph representing the wing area (pixels $\times 10^4$) of flies of the indicated genotypes (n = 20 of each genotype). D) ab^1; *ab-GFP/+* wing. Note the rescue of the L5 vein length and the size of the wing. E) Graph representing the wing area (pixels $\times 10^4$) of flies of the indicated genetic backgrounds (n = 20 of each genotype). Note the rescue of ab^1 wing size in the presence of the *ab* genomic duplication (*ab-GFP*). E′) Graph representing the wing area (pixels) of flies of the indicated genotypes (n = 20 of each genotype). F) *sdG4/+; UAS GFP/+* wing imaginal disc showing GFP expression (green) indicating the expression domain of the *sdG4* line, mainly in the wing pouch area of the wing disc (arrowhead). G) *sdG4/+; UAS GFP/+* wing used as a control. H) *sdG4/+; UAS abrupt*$_{RNAi}$*/+* wing. I) Graph representing the wing area of flies of the indicated genotypes (n = 20 of each genotype). J) Wing imaginal disc showing Abrupt expression pattern. Note that Abrupt expression is detected in the wing pouch and *notum* regions and in the veins primordia as previously described (Cook et al., 2004) (asterisk indicating the L5 vein primordium). K, L) Wing area between L3 and L5. The black square identifies an example of the areas chosen to calculate trichome density. (K) control wing (y^1w^{1118}). (L) ab^1 homozygous wing. M) Graph representing the trichome density in control and in homozygous ab^1 wings (n = 20 of each genotype). N) Graph representing the wing area (pixels) of flies of the indicated genotypes (n = 20 of each genotype). Scale bars represent 500 µm for wings and 50 µm for wing discs and wings enlargements. Asterisks denote the following p values: 0.01 < *p < 0.05, 0.001 < p** < 0.01, ***p < 0.001.

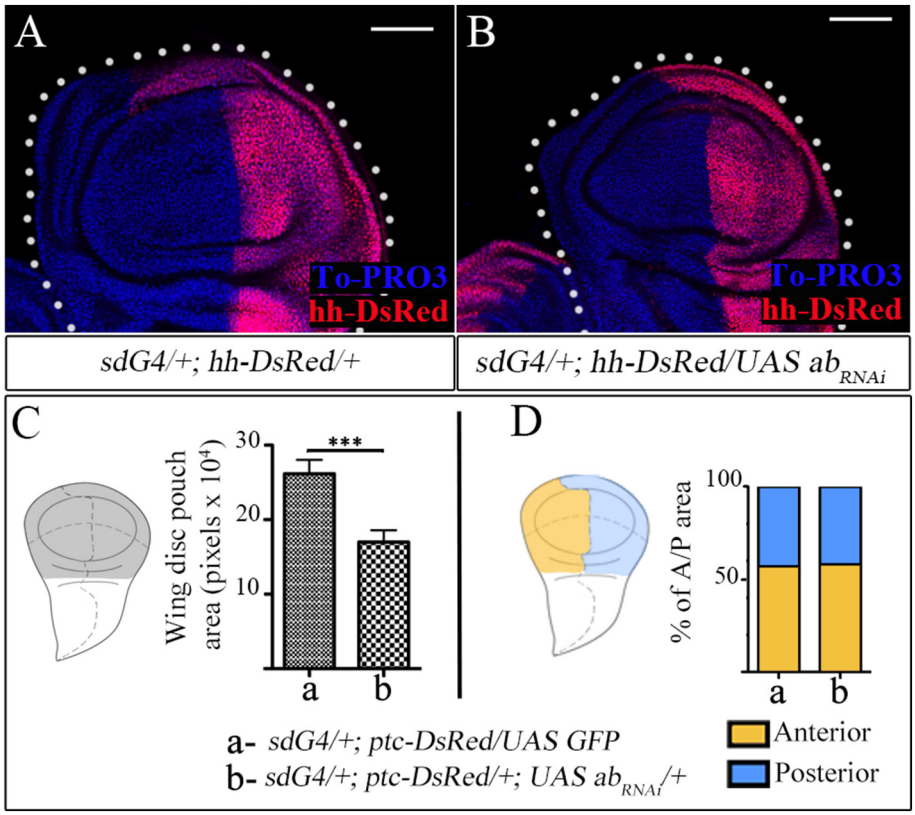

Fig. 2. Inactivation of *abrupt* causes a reduction in wing disc size. A) *sdG4/+; ptc-DsRed/UAS GFP* wing disc (used as a control) showing *ptc-DsRed* expression (red) and To-PRO3 (blue). B) *sdG4/+;ptc-DsRed/+; UAS* ab_{RNAi}*/+* wing disc showing *ptc-DsRed* expression (red) and To-PRO3 (blue). Note the reduction of wing disc size compared to (A). C) *sdG4/+; hh-DsRed/+* wing disc (used as a control) showing *hh-DsRed* expression (red) and To-PRO3 (blue). D) *sdG4/+;hh-DsRed/UAS* ab_{RNAi} wing disc showing *hh-DsRed* expression (red) and To-PRO3 (blue). Note the reduction of wing disc size compared to (C). E) Diagram of a wing disc indicating the domain of *sdG4* expression in the wing pouch region (grey) used for area measurements. The graph represents the area (pixels $\times 10^4$) of the indicated genotypes (a = *sdG4/+; ptc-DsRed/UAS GFP*, b = *sdG4/+; ptc-DsRed/+; UAS* ab_{RNAi}*/+*) (n = 15 of each genotype). F) Diagram of a wing disc indicating the anterior (A, orange) and the posterior (P, blue) compartments in the wing pouch and the *ptc-DsRed* (red) indicating the A/P boundary. Graph representing the percentage (%) of the A and P compartment areas (pixels $\times 10^4$) within the wing discs of the indicated (a and b) genotypes (n = 15 of each genotype). Note that the percentage of area occupied by either the A or the P compartments in (a) is similar to the corresponding area in (b), indicating that the wing disc reduction impacts proportionally both compartments. Scale bars represent 50 μm for wing discs. Asterisks denote the following p values: ***p < 0.001.

compartments size measurements, the posterior border of ptc-DsRed expression was used as a marker of the A/P compartment boundary.

3. Results

3.1. The inactivation of abrupt function reduces the size of both the wing and the wing disc

We first studied wing size changes resulting from the inactivation of *abrupt* function (Fig. 1) using different mutant alleles such as ab^1 (Morgan et al., 1925), $ab^{EY01129}$ and ab^{clu1} (Vactor et al., 1993) as well as the *UAS* $abrupt_{RNAi}$ line that efficiently inactivates the expression of *abrupt* (Supplementary Fig. 1). We found that homozygous flies ab^1, $ab^{EY01129}$, ab^{clu1} flies show a significant reduction of wing size when compared to control y^1w^{1118} flies (Fig. 1A–C). Additionally, these mutant flies show the shortening of the L5 vein previously reported (Fig. 1B) (Cook et al., 2004; Hu et al., 1995). Depending on the *abrupt* mutant allele combination, the degree of wing reduction ranged from 10 to 25%, and in all cases the reduction was statistically significant (Fig. 1C). Importantly, the reduced wing size and L5 vein length is rescued with a genomic duplication of the *ab* gene (*ab-GFP*, see Material and methods) as the size of the wings from ab^1*; ab-GFP/+* flies is identical to control wings (Fig. 1D, E′). This strongly suggests that the observed wing size reduction is due to *abrupt* inactivation.

Moreover, when we inactivated the expression of *abrupt* using the *scalloped Gal4* (*sdG4*) line that drives the expression in the wing pouch region (Fig. 1F) in combination with the *UAS* $abrupt_{RNAi}$ (*UAS* ab_{RNAi}) line, we found that *sdG4/+;UAS* ab_{RNAi}*/+* wings are also significantly smaller than the control *sdG4/+;UAS GFP/+* wings (Fig. 1G–I). These results indicate that lack of *abrupt* function affects wing growth, a function not previously attributed to this gene. Because of the effect of *abrupt* inactivation on the overall size of the wing, we analyzed *abrupt* pattern of expression using anti-Abrupt antibody (Hu et al., 1995). We found that Abrupt protein is detectable not only in the vein primordial cells, as previously reported using RNA probes (Cook et al., 2004), but also in the majority of the wing disc cells both in the wing pouch and the *notum* (Fig. 1J).

To characterize the role of *abrupt* in the control of wing growth, we analyzed whether the wing size reduction is a consequence of decreased cell size by measuring trichome density. In the wing, each cell contains one trichome (Robertson, 1959) and thus the analysis of the number of trichomes per area is an indication of the cell size. We quantified trichome density in wings of ab^1 flies compared to the wings of control flies (Fig. 1K, L). This comparison shows an increase in trichome density in ab^1 wings over that seen in control wings (Fig. 1M). This result indicates that the size of ab^1 wing cells is reduced and suggests that the reduction of wing size is associated with reduction of wing cells size. We then analyzed whether apoptosis was also involved in the wing size reduction observed when *abrupt* function is inactivated. For that, we inhibited apoptosis by overexpression of DIAP1 (Drosophila Inhibitor of Apoptosis 1 (Hay et al., 1995)). We found that *sdG4/+; UAS DIAP1/+; UAS* ab_{RNAi}*/+* wings have a larger size than *sdG4/+; UAS GFP/+; UAS* ab_{RNAi}*/+* flies (Fig. 1N). Thus, both reduction of wing cells size as well as cell death are involved in the reduction of wing size upon *abrupt* inactivation.

We then investigated the induction of apoptosis during wing disc development by monitoring activated Caspase-3 (C3) levels of expression. Neither homozygous ab^1 wing discs nor wing imaginal discs from *sdG4/+;UAS* ab_{RNAi}*/+* larvae showed expression of C3 (Supplementary Fig. 3) indicating that inactivation of *abrupt* function during larval development does not activate cell death at detectable levels. We therefore investigated whether the size reduction occurs before or after metamorphosis by comparing the size of wing imaginal discs.

To better visualize and compare the size and effects on disc morphology, we used the markers *patched-DsRed* (*ptc-DsRed*, see Material and methods) and *hedgehog-DsRed* (*hh-DsRed*, see Material and methods) (Akimoto et al., 2005). Wing imaginal discs *sdG4/+; ptc-DsRed/UAS GFP* (Fig. 2A) are larger than *sdG4/+; ptc-DsRed/+; UAS* ab_{RNAi}*/+* wing discs (Fig. 2B). Likewise, wing discs *sdG4/+; hh-DsRed/*

+ (Fig. 2C) are larger than *sdG4/+; hh-DsRed/UAS ab$_{RNAi}$* (Fig. 2D).

We then analyzed whether inactivation of *abrupt* impacts the size of the anterior (A) and posterior (P) wing disc compartments. For that, we used experimental wing discs (*sdG4/+; ptc-DsRed/+; UAS ab$_{RNAi}$/+*) and control wing discs (*sdG4/+; ptc-DsRed/UAS GFP*) where the expression of *ptc-DsRed* was indicative of the location of the A/P compartment boundary. We first found that inactivation of *abrupt* produces a 35% reduction of the whole wing pouch disc size, compared to control wing discs (Fig. 2E). Also, we found that in control wing discs (*sdG4/+; ptc-DsRed/UAS GFP*), the A compartment occupies 57% of the total area and that the P compartment occupies the remaining 43% of the total area. Furthermore, we found that in wing discs where *abrupt* was inactivated (*sdG4/+; ptc-DsRed/+; UAS ab$_{RNAi}$/+*) the A compartment occupies 58% of the total area and the P compartment occupies 42% of the total area (Fig. 2F). Thus, inactivation of *abrupt* in the whole wing pouch influences proportionally the reduction of the A and P compartments.

Taken together these results show that *abrupt* inactivation results in the reduction of wing and wing disc size indicating a role of *abrupt* in size control.

3.2. The inactivation of abrupt function influences haltere size

While analyzing the function of *abrupt* in the control of wing size, we noticed that inactivation of *abrupt* influenced on leg size (Supplementary Fig. 2) as previously described (Hu et al., 1995) and curiously on haltere size. This prompted us to study the function of *abrupt* inactivation in haltere development. We first studied the pattern of Abrupt protein expression in the haltere disc and found that it is detected in nearly all the cells of the disc (Fig. 3A), showing a stronger expression in the region of the haltere disc pouch that will give rise to the *capitellum* (Fig. 3B). Next, we analyzed the size and morphology of the halteres of homozygous *ab^{1}* flies and found that these display smaller halteres (Fig. 3C) than control flies (Fig. 3B). Using the *sdG4* line that drives the expression in the haltere disc pouch (Fig. 3D), we also found that *sdG4/+;UAS ab$_{RNAi}$/+* flies show smaller halteres (Fig. 3E) than control *sdG4/+;UAS GFP/+* flies (Fig. 3B). Haltere size is difficult to measure due to its balloon-like morphology. However, most cases of small halteres displayed a longitudinal indentation (Fig. 3C, E) resembling a "heart", a morphological feature that we named "heart-shaped halteres" that can be visually quantified and used as a measure of the severity of the phenotype. Using this measure roughly 80% of the halteres of homozygous *ab^{1}* flies and 78% of *sdG4/+; UAS ab$_{RNAi}$/+* flies are "heart-shaped" (Fig. 3F) and, therefore, exhibit severely reduced size.

We next studied the size of the complete haltere disc pouch as well as the size of the haltere disc pouch anterior (A) and posterior (P) compartments. For this, we used the *sdGal4* line (Fig. 3D) and the *ptc-DsRed* (Fig. 3G) and the *hh-DsRed* (Fig. 3I) expression patterns as markers of the haltere A and P compartments. We found that inactivation of *abrupt* expression in the whole haltere pouch (*sdG4/+; ptc-DsRed/+; UAS ab$_{RNAi}$/+* (Fig. 3H) and *sdG4/+; hh-DsRed/UAS ab$_{RNAi}$* (Fig. 3J)) produces a reduction of the size of the haltere disc compared to control haltere discs (*sdG4/+; ptc-DsRed/+* (Fig. 3G) and *sdG4/+; hh-DsRed/+* (Fig. 3I)). We calculated the reduction and found that inactivation of *abrupt* produces a 30% reduction of the haltere pouch (Supplementary Fig. 4). Further, we found that both in control (*sdG4/+; ptc-DsRed/+*) and mutant (*sdG4/+; ptc-DsRed/+; UAS ab$_{RNAi}$/+*) discs, the A compartment occupies 77% of the haltere disc area and the P compartment occupies 23% of the haltere disc area, indicating that the reduction of the haltere size impacts the A and P compartments equally and proportionally (Supplementary Fig. 4). However, this reduction of the haltere disc is not related with apoptosis induction as activation of Caspase-3 expression was not seen in *sdG4/+;UAS ab$_{RNAi}$/+* haltere discs (data not shown).

Taken together, these results indicate that *abrupt* controls haltere size in a similar way to the way it controls wing size.

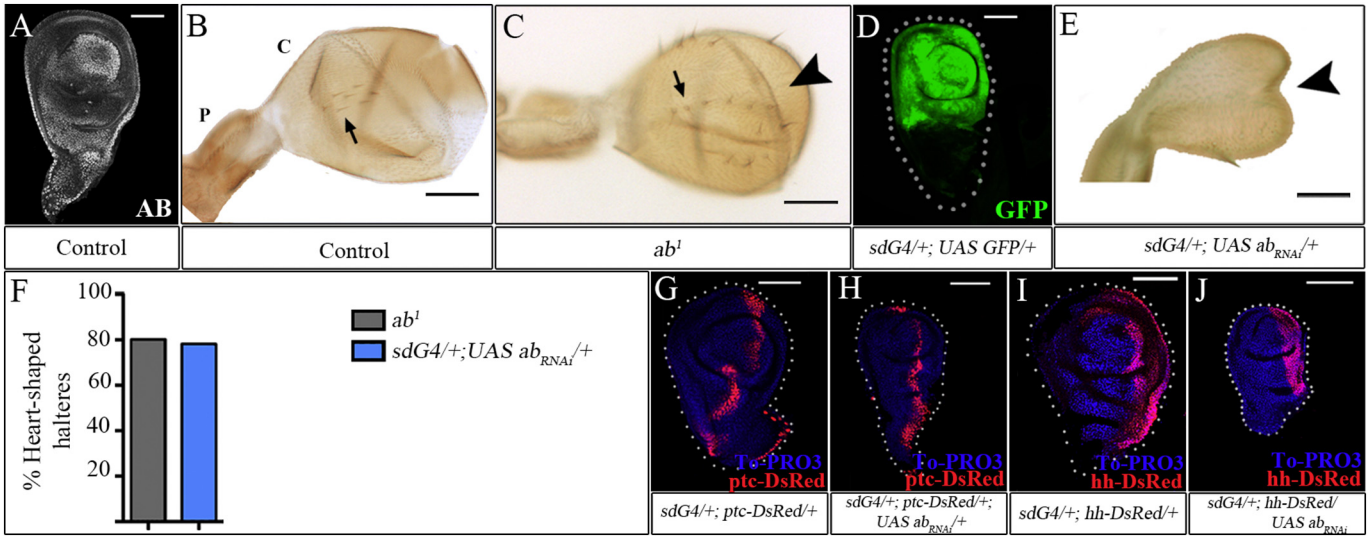

Fig. 3. Inactivation of *abrupt* function causes a reduction in haltere size. A) Control *sdG4/+; UAS GFP/+* haltere disc showing Abrupt expression. Note that Abrupt expression is detected in almost all the haltere disc cells. B) *y^{1}w^{1118}* haltere used as a control (c: *capitelum*, p: *pedicelum*) containing trichomes covering the entire haltere and the sensilla trichodea (arrow). C) Homozygous *ab^{1}* haltere containing the trichomes covering the entire haltere and sensilla trichodea (arrow). Note the reduction of size compared to (B) and the appearance of an indentation (arrowhead). D) *sdG4/+; UAS GFP/+* haltere disc, used as control disc, showing the *sdG4* domain of expression (GFP). E) *sdG4/+; UAS ab$_{RNAi}$/+* haltere. Note the reduction of haltere size and the appearance of the indentation (arrowhead) that generates a "heart-shaped" haltere. F) Graph representing the percentage of "heart-shaped" halteres of the indicated genotypes, (n = 80 for *ab^{1}*, n = 50 for *sdG4/+; UAS ab$_{RNAi}$/+*). G) *sdG4/+; ptc-DsRed/+* haltere disc showing the expression of To-PRO3 (blue) and of *ptc-DsRed* (red) in the anterior compartment at the A/P boundary. H) *sdG4/+; ptc-DsRed/+; UAS ab$_{RNAi}$/+* haltere disc showing the expression of To-PRO3 (blue) and of *ptc-DsRed* (red). Note the reduction of the haltere disc size compared to (G). I) *sdG4/+; hh-DsRed/+* haltere disc showing the expression of To-PRO3 (blue) and of *hh-DsRed* (red) in the posterior compartment. J) *sdG4/+; hh-DsRed/UAS ab$_{RNAi}$* haltere disc showing the expression of To-PRO3 (blue) and of *hh-DsRed* (red) in the posterior compartment and To-PRO3 (blue).

3.3. Analysis of abrupt and Ultrabithorax genetic interaction

Reduced haltere size has been previously associated with inactivation of the *decapentaplegic* (*dpp*) morphogen and/or overexpression of a variety of factors such as the homeotic gene *Ultrabithorax* (*Ubx*) (de Navas et al., 2006; Roch and Akam, 2000; Simon and Guerrero, 2015). This led us to analyze the genetic interaction between *abrupt* and *Ubx* genes. The UBX protein is detected in all haltere disc cells being strongly expressed in the haltere pouch (Fig. 4A, Smolik-Utlaut, 1990). We analyzed UBX protein levels using different *Gal4* lines such as *sdG4*,

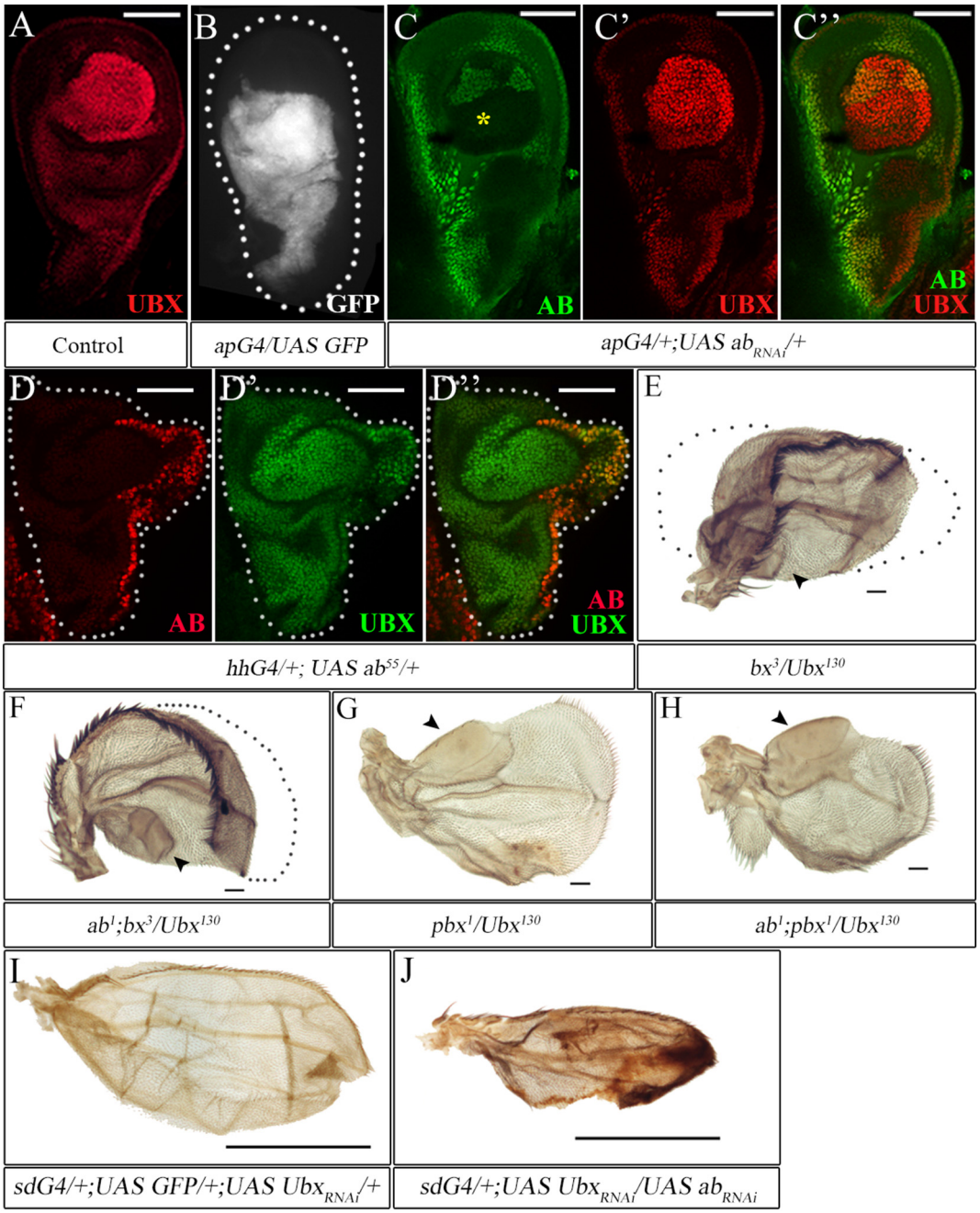

Fig. 4. Analysis of *abrupt* and *Ultrabithorax* genetic interaction. A) Control y^1w^{1118} haltere disc showing the expression of UBX (green). B) *apG4/UAS GFP* haltere disc showing the *apG4* domain of expression (grey) in the dorsal compartment of the disc. C–C″) *apG4/+; UAS* ab_{RNAi}/+ haltere disc showing the expression of (C) Abrupt (AB, green), (C′) UBX (red) and (C″) merged image. Note that Abrupt expression disappears in the dorsal compartment (C, asterisk) while UBX expression (C′) is not altered. D–D″) *hhG4/+; UAS* ab^{55}/+ haltere disc showing (D) AB expression (green), (D′) UBX expression (red) and (D′) merged image. Note the overgrowths and that high levels of AB do not modify UBX levels. Also note that the endogenous levels of AB are weak due to the focus on the overgrowths. E) Haltere bx^3/Ubx^{130} showing the transformation of the anterior compartment towards wing. The posterior compartment (arrowhead) is not affected. F) Haltere $ab^1;bx^3/Ubx^{130}$ showing the transformation of the anterior compartment towards wing. The posterior compartment (arrowhead) is not affected. The dotted lines represent the "unfolded" transformed wing area which covers a smaller area in (F) than (E) due to the presence of ab^1. G) Haltere pbx^1/Ubx^{130} showing the transformation of the posterior compartment towards wing. The anterior compartment (arrowhead) is not affected. H) Haltere $ab^1;pbx^1/Ubx^{130}$ showing the transformation of the posterior compartment towards wing. The posterior compartment (arrowhead) is not affected. Note that the posterior transformed compartment in (H) is smaller than the corresponding one in (G) due to the presence of ab^1. I) Haltere *sdG4/+; UAS GFP/+; UAS* Ubx_{RNAi}/+ showing a transformation of both the A and P compartments towards wing. J) Haltere *sdG4/+; UAS* Ubx_{RNAi}/*UAS* ab_{RNAi} showing the transformation of both the A and P compartments towards wing. Note that the size of (J) is smaller than (I) due to *abrupt* inactivation. Scale bars represent 50 μm for wing discs and halteres.

hhG4 and *apG4* and the *UAS abrupt$_{RNAi}$* line. The *apG4* line directs transgene expression in the haltere disc dorsal cells (Fig. 4B). We observed that the inactivation of *abrupt* in *apG4/+; UAS ab$_{RNAi}$/+* haltere discs efficiently reduces Abrupt expression in the dorsal cells (Fig. 4C) but does not affect UBX levels (Fig. 4C′, C″), indicating that *abrupt* does not regulate the expression of *Ubx*. We next analyzed whether *abrupt* could negatively regulate the expression of *Ubx* by analyzing the effect of high levels of Abrupt on UBX levels. Haltere imaginal discs *sdG4/+;UAS ab^{55}/+* showed overgrowths (Fig. 4D) similar to the reported effect of high levels of Abrupt in wing imaginal cells (Turkel et al., 2013) but they did not show an effect on UBX levels of expression (Fig. 4D–D″). Moreover, overexpression of UBX in *ciG4/UAS Ubx; tub Gal80^{ts}/+* in the wing imaginal discs did not influence the levels of Abrupt (Supplementary Fig. 5). Thus, these results suggest that Abrupt does not control *Ubx* expression and that UBX does not control *abrupt* expression.

We then studied the genetic interaction between *abrupt* and *Ubx* using the *bx^3* and *pbx^1* mutations of the *Ubx* gene that specifically and respectively inactivate *Ubx* expression in the anterior (A) and posterior (P) compartments. We also used the *UAS Ubx$_{RNAi}$* line in combination with *sdG4*. As previously reported, the inactivation of *Ubx* in the A compartment of the haltere disc (*bx^3/Ubx^{130}*) produced flies with the A compartment of the haltere transformed towards the A compartment of the wing (Fig. 4E) (Bender et al., 1983; Casanova et al., 1985). Moreover, inactivation of *Ubx* in the haltere disc P compartment (*pbx^1/Ubx^{130}*) produced flies with the P compartment of the haltere transformed towards the P compartment of the wing (Fig. 4G) (Bender et al., 1983; Casanova et al., 1985). We then analyzed these homeotic transformations in the absence of *abrupt*. Flies *ab^1; bx^3/Ubx^{130}* (Fig. 4F) as well as flies *ab^1; pbx^1/Ubx^{130}* (Fig. 4H) show the corresponding homeotic transformation. Notably, the size of the transformed A compartment in *ab^1; bx^3/Ubx^{130}* was smaller than the transformed A compartment in *bx^3/Ubx^{130}* flies (compare the extent of the dotted lines in Fig. 4E *versus* Fig. 4F). Furthermore, the transformed P compartment was smaller in *ab^1; pbx^1/Ubx^{130}* flies than the transformed P compartment of *pbx^1/Ubx^{130}* flies (compare the P compartments in Fig. 4G and H). Similar differences in the sizes of the transformed wings were also observed comparing wings expressing *abrupt* (*sdG4/+;UAS GFP/+; UAS Ubx$_{RNAi}$/+*) to wings not expressing *abrupt* (*sdG4/+;UAS Ubx$_{RNAi}$/UAS ab$_{RNAi}$*, Fig. 4I–J).

Thus, the results from this analysis of the genetic interaction between *abrupt* and *Ubx* indicates that Abrupt does not regulate *Ubx* expression nor does UBX regulates *abrupt* expression. However, these results do support the proposition that *abrupt* is required for growth.

3.4. The microRNA miR-306 regulates abrupt expression to control wing and haltere size

To investigate the regulatory pathway through which *abrupt* controls growth we searched for upstream regulators of *abrupt* as well as for downstream *abrupt* effectors. The analysis of the *abrupt* gene 3′-UTR identified the existence of a *miR-306* binding site (Fig. 5A) (http://www.targetscan.org/fly), suggesting that *abrupt* is directly regulated by *miR-306*. We first checked whether the *3′-UTR-abrupt-GFP* (*3′-UTR-ab-GFP* sensor construct (Okamura et al., 2008)) was responsive to high levels of *miR-306*. For that, we generated *UAS miR-306-DsRed* constructs and the corresponding transgenic lines to analyze the expression of *3′-UTR-ab-GFP* in wing imaginal discs expressing high levels of *miR-306*. Wing imaginal discs containing the *3′-UTR-ab-GFP* showed ubiquitous GFP expression (Fig. 5B). However, *ptcG4/3′UTR ab-GFP;UAS miR-306^{20}-DsRed/+* wing imaginal discs where *miR-306* is overexpressed under the control of *ptcG4* showed repression of GFP expression throughout the *ptcG4* domain (Fig. 5C–C″), indicating that *miR-306* acts on *abrupt* 3′-UTR to repress its expression. Next, we checked whether Abrupt protein levels were changed in wing imaginal discs containing high levels of *miR-306*. Abrupt is expressed in nearly all the cells of the wing pouch in wild type wing imaginal discs (Fig. 5D). In *hhG4/UAS miR-306^{20}-DsRed* wing imaginal discs, the levels of Abrupt are diminished in the posterior compartment cells corresponding to the *hhG4* domain when compared to Abrupt levels in the anterior compartment cells (Fig. 5E–E″). These results further suggest that *miR-306* directly regulates *abrupt* expression levels.

To investigate whether *miR-306* functions together with *abrupt* in the control of the wing and haltere growth, we studied the phenotypic effect of overexpression of *miR-306* in the wing and haltere as well as the genetic interaction between *abrupt* and *miR-306*. Overexpression of *miR-306* in larvae grown at 25 °C using the *sdG4* line (*sdG4/+; UAS miR-306^{20}-DsRed/+*) resulted in flies with wings of smaller size (Fig. 5F) than control wings (*sdG4/+; UAS GFP/+*, Fig. 5H) and notably, with L5 of a shorter length than controls (Fig. 5F). Each of these phenotypes is associated with the inactivation of *abrupt* as shown in Fig. 1B and H. Moreover, the overexpression of *miR-306* in larvae grown at 29 °C (*sdG4/+; UAS miR-306^{20}-DsRed/+*) resulted in flies with small halteres (Fig. 5G) a phenotype similar to that seen with the inactivation of *abrupt* (Fig. 3C, E). Thus, *miR-306* overexpression produces flies with wing and haltere phenotypes similar to flies where the function of *abrupt* is inactivated, supporting a role for *miR-306* in the negative regulation of *abrupt* expression.

We next studied the genetic interaction between *miR-306* and *abrupt* in a double heterozygous assay. We used the *ab^1* mutant allele and the genomic deletion *miR-306-79-9b-KO* that removes *miR-306* and the *miR-79* and *miR-9b* loci (Chen et al., 2014). Of note, the reduction of wing size observed when *miR-306* is overexpressed (*sdG4/+; UAS miR-306^{20}-DsRed/+*) (Fig. 5F) is modulated in homozygous *miR-306-79-9b-KO* flies (*sdG4/+; miR-306-79-9b-KO; UAS miR-306^{20}-DsRed/+*, Supplementary Fig. 6) supporting the function of *miR-306* in wing size control.

Flies *ab^1* heterozygous (*ab^1, miR-306^{wt}/ab^{wt}, miR-306^{wt}*) presented wings of normal size (not shown) while flies *ab^1* homozygous (*ab^1, miR-306^{wt}/ab^1, miR-306^{wt}*) presented wings of reduced size (Fig. 1C). Moreover, flies *miR-306-79-9b-KO* heterozygous (*ab^{wt}, miR-306-79-9b-KO/ab^{wt}, miR-306^{wt}*) showed wings of normal size (data not shown) while flies *miR-306-79-9b-KO* homozygous (*ab^{wt}, miR-306-79-9b-KO/ab^{wt}, miR-306-79-9b-KO*) flies presented wings of reduced size (Supplementary Fig. 7). We analyzed the size of wings from flies double heterozygous for *ab^1* and *miR-306-79-9b-KO* (*ab^1, miR-306^{wt}/ab^{wt}, miR-306-79-9b-KO*) and found that they are of similar size as wings from flies *ab^1* homozygous (*ab^1, miR-306^{wt}/ab^1, miR-306^{wt}*) (Fig. 5J). This result indicates a genetic interaction between *miR-306* and *abrupt* to control wing size.

Thus, the analyses of *miR-306* function in the regulation of *abrupt* suggest that *miR-306* regulates the expression of *abrupt* and that *miR-306* and *abrupt* collaborate to control the size of both wing and haltere.

3.5. Cyclin E and dacapo collaborate with abrupt to regulate wing and haltere size

Previous transcriptome analysis results from eye-imaginal discs containing high levels of Abrupt indicate that Abrupt regulates the expression of genes essential for cell cycle progression (Turkel et al., 2013). Because of this, we chose to investigate whether *Cyclin E* and *dacapo* contribute to the wing and haltere size control mediated by *abrupt*. Cyclin E functions together with the cdk2 kinase to promote the G1-S transition (Richardson et al., 1995). However, Dacapo inhibits cell cycle progression by binding to the CycE-cdk2 complex and impeding the G1-S transition (de Nooij et al., 1996; Lane et al., 1996).

To study the epistatic relationships between *Cyclin E* and *dacapo* with *abrupt* in the control of wing size, we analyzed the effect of overexpression of *Cyclin E* as well as the inactivation of *dacapo* on the wing size produced by *abrupt* inactivation. The concomitant overexpression of *Cyclin E* and inactivation of *abrupt* (*sdG4/+;UAS Cyclin E/+;UAS ab$_{RNAi}$/+*) produced flies with wings of larger size than those of

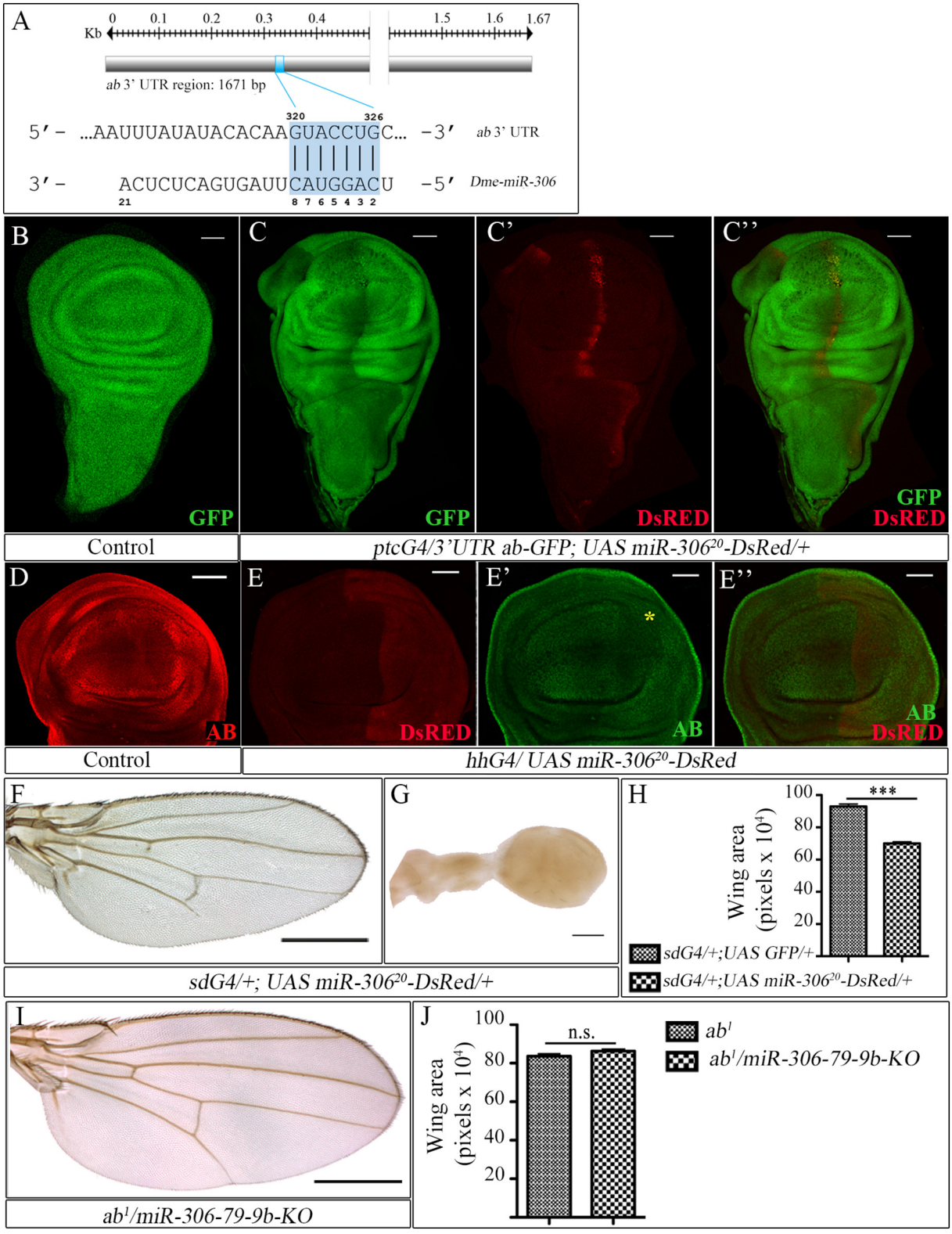

(caption on next page)

flies where only *abrupt* expression was inactivated (*sdG4/+;UAS GFP/+; UAS* ab_{RNAi}/+) (Fig. 6A–C). This result indicates that high levels of *Cyclin E* rescues the wing size reduction associated with the inactivation of *abrupt*, thereby suggesting that *Cyclin E* functions together with *abrupt* to control wing size. Interestingly, the shortening of the L5 vein associated with *abrupt* inactivation was also rescued in the presence of high levels of *Cyclin E* (Fig. 6B, F) supporting the results showing that *Cyclin E* and *abrupt* contribute together to control wing size.

We next investigated the effect of *dacapo* inactivation on the wing size produced by *abrupt* inactivation. The concomitant inactivation of *dacapo* and *abrupt* (*sdG4/+;UAS* ab_{RNAi}/*UAS* dap_{RNAi}) (Fig. 6D) resulted in flies with wings of larger size than wings from flies where only *abrupt*

Fig. 5. The microRNA *miR-306* regulates *abrupt* expression to control wing and haltere size.
A) Abrupt is a predicted target of *miR-306*. Scheme of the *ab* 3′UTR (1671 bp) showing the seed sequence of *miR-306* (at position 320–326) that has complementarity with the ab 3′UTR (http://www.targetscan.org/fly). B) Wing disc *3′UTR-ab-GFP* showing GFP (green) expression. C–C″) Wing disc *ptcG4/3′UTR ab-GFP; UAS miR-306^{20}-DsRed/+* showing GFP expression (green) (C) and DsRed expression (red) (C′). (C″) Merge image of (C) and (C′). D) Wing pouch region of a control (y^1w^{1118}) wing disc showing Abrupt expression (red) in the cells of the vein primordial as well as the wing pouch cells. E–E″) Wing pouch region of a *hhG4/UAS miR-306^{20}-DsRed* wing disc showing the expression of DsRed (E, red) and Abrupt (E′, green). Note the decreased Abrupt expression (green) (asterisk). (E″) Merge image of (E) and (E′). F) Wing *sdG4/+; UAS miR-306^{20}-DsRed/+* grown at 25 °C. Note the decrease in size compared to Fig. 1A Graph representing and the L5 shortening. G) *sdG4/+; UAS miR-306^{20}-DsRed/+* haltere grown at 25 °C. Note the decrease in size compared to Fig. 3B. H) Graph representing the wing area (pixels $\times 10^4$) of the indicated genotypes (n = 20 of each genotype). I) Wing *ab^1/miR-306-79-9b-KO*. J) Graph representing the wing area of the indicated genotypes (n = 20 for each genotype). Note that there are no significant differences in the size of the wing in both genotypes. Scale bars represent 50 μm for wing discs and halteres and 500 μm for wings. n.s. - not significant, *** $p < 0.001$.

expression is inactivated (*sdG4/+;UAS GFP/+;UAS ab$_{RNAi}$/+*) (Fig. 6E) indicating that low levels of *dacapo* rescues the wing size reduction associated with *abrupt* inactivation. Also in this case, the L5 vein shortening associated with *abrupt* inactivation was rescued in the absence of *dacapo* expression (Fig. 6A, F). Taken together, these results suggest that *abrupt* regulates wing size in collaboration with *Cyclin E* and *dacapo*.

We further analyzed the epistatic relationships between *Cyclin E* and *dacapo* with *abrupt* in the control of haltere size. To analyze haltere size, we used two parameters: percentage of the "heart-shaped" halteres and the expression of the ptc-DsRed and hh-DsRed reporters in the halteres (Fig. 6G–H) whose patterns of expression were not affected by either overexpression of Cyclin E or by inactivation of *dacapo* (Supplementary Fig. 8). Overexpression of *Cyclin E* (*sdG4/+;UAS Cyclin E/+;UAS ab$_{RNAi}$/+*) rescued the expression of *ptc-DsRed* and *hh-DsRed* when compared with (*sdG4/+;UAS GFP/+;UAS ab$_{RNAi}$/+*) (Fig. 6I–L). However, and curiously, although *sdG4/+;UAS Cyclin E/+;UAS ab$_{RNAi}$/+* halteres were significantly larger than control halteres, the percentage of heart-shaped halteres was not affected. Finally, inactivation of *dacapo* (*sdG4/+;ptc-DsRed/+;UAS ab$_{RNAi}$/UAS dap$_{RNAi}$*) reduced the percentage of heart-shaped halteres (Fig. 6M) and rescued the expression of *hh-DsRed* when compared with (*sdG4/+;UAS GFP/+;UAS ab$_{RNAi}$/+*) (Fig. 6N). Thus, these results indicate that *abrupt* controls haltere size in collaboration with cell cycle regulators such as *Cyclin E* and *dacapo*.

4. Discussion

Understanding how an organ initiates growth and then stops growing when its final size and shape is achieved is a fundamental question in developmental biology. Despite the extensive knowledge concerning the cellular, mechanical and molecular mechanisms regulating growth, how the growth and patterning of developing organs are controlled and coordinated is still a standing question. Cross-species conservation of the molecular pathways makes *Drosophila* an excellent model system for the analysis of growth control. In particular, the use of the wing and haltere imaginal discs - that give rise to the adult wings and halteres - have served to reveal fundamental aspects of growth and development (Day and Lawrence, 2000; Mirth and Shingleton, 2012; Restrepo et al., 2014; Teleman and Cohen, 2000).

In this work, we have analyzed the function of *abrupt* (*ab*) in the control of wing and haltere size. We have discovered that the *abrupt* gene is required in both the wing and the haltere to achieve their normal size (Figs. 1 and 2). This novel function of *abrupt* adds to the previously described *abrupt* functions in the determination of the L5 wing vein, in motoneuronal branching, border cell migration as well as leg development (Cook et al., 2004; Hu et al., 1995; Jang et al., 2009; Hattori et al., 2013; Li et al., 2004; Sugimura et al., 2004). We found that Abrupt, in addition to the previously reported expression in the primordial cells of the L5 vein (Cook et al., 2004), is expressed in nearly all cells of both wing (Fig. 1J) and haltere imaginal discs (Fig. 3A), supporting our proposal that *abrupt* controls the overall size of these appendages. The amount of wing size reduction observed in *ab* mutants or when *ab* is inactivated ranges from 7 to 22% of total (Fig. 1C, I). This reduction may seem small but is statistically significant and, moreover, is rescued with a duplication of the *abrupt* gene (Fig. 1D–E′), and modulated in several genetic backgrounds (Fig. 6B, D). The quantification of wing trichomes (Fig. 1M) indicates that the reduction of wing size is related to the reduction of cell size. Also, the reduction of wing size may be due to apoptosis during pupal development (Fig. 1N). Curiously, this apoptosis does not occur during larval development (Supplementary Fig. 3).

Whether, in addition to control cell size *abrupt* is also controlling cell numbers and cell proliferation is still to be determined. Interestingly, the size reduction due to inactivation of *abrupt* is already detected in the wing imaginal discs (Fig. 2) and impacts equally the anterior and the posterior compartments, indicating that *abrupt* controls the overall size of the wing rather than the size of a specific compartment. This function of *abrupt* is novel and in addition to contributing to the understanding of growth control, contributes to our understanding of the coordination of growth and pattern, *i.e.* how the overall growth of the wing might also control the growth of region specific patterns such as veins.

Interestingly, the role of *abrupt* in growth control is not restricted to wing development but also influences haltere development. Our results show that inactivation of *abrupt* produces halteres of smaller size than control halteres (Fig. 3C, E, F) and that this reduction is already detected in the haltere imaginal disc (Fig. 3H, J). The analysis of *ptc-DsRed* and *hh-DsRed* reporters during the development of the haltere indicates that, as in the wing, *abrupt* controls the size of the entire haltere rather than controlling the size of either the anterior or the posterior compartments (Fig. 3G–J, Supplementary Fig. 4), supporting a role for *abrupt* in the global control of growth. Also, the fact that both reporters can be detected in the haltere (Fig. 6G–H) may be useful to more accurately and spatially fate map the position of specific bristles and sensillas to haltere compartments (Gonzalez-Gaitan et al., 1990). Finally, we do not understand the cause of the indentation seen in halteres expressing low levels of *abrupt*. Further investigation is needed to understand the origin of this phenotype and how it relates haltere morphogenesis.

Data from other laboratories have suggested a genetic interaction between *abrupt* and *Ubx* genes (Choo et al., 2011; Pavlopoulos and Akam, 2011). It has been found that the UBX protein binds to *abrupt* regulatory sequences (Choo et al., 2011) and that *abrupt* expression is up-regulated when UBX is overexpressed in pre-pupa and pupa stages (Pavlopoulos and Akam, 2011). The *Ubx* gene controls the size of the haltere by repressing the expression of *Dpp* and its downstream effector genes. Indeed, either high levels of UBX or inactivation of *Dpp* function in the haltere produce the reduction of its size (de Navas et al., 2006). Our work shows that high levels of UBX do not alter the expression of Abrupt in the wing and haltere imaginal discs (Supplementary Fig. 5) nor do low (Fig. 4C) or high (Fig. 4D) levels of Abrupt alter UBX expression. Thus, *abrupt* and *Ubx* do not seem to interact during larval development. Perhaps the interaction takes place during pupal development (Pavlopoulos and Akam, 2011). Nevertheless, our analysis of the genetic interactions between *Ubx* and *abrupt* supports a role for *abrupt* in growth (Fig. 4E–J).

A number of microRNAs have been found to influence wing size

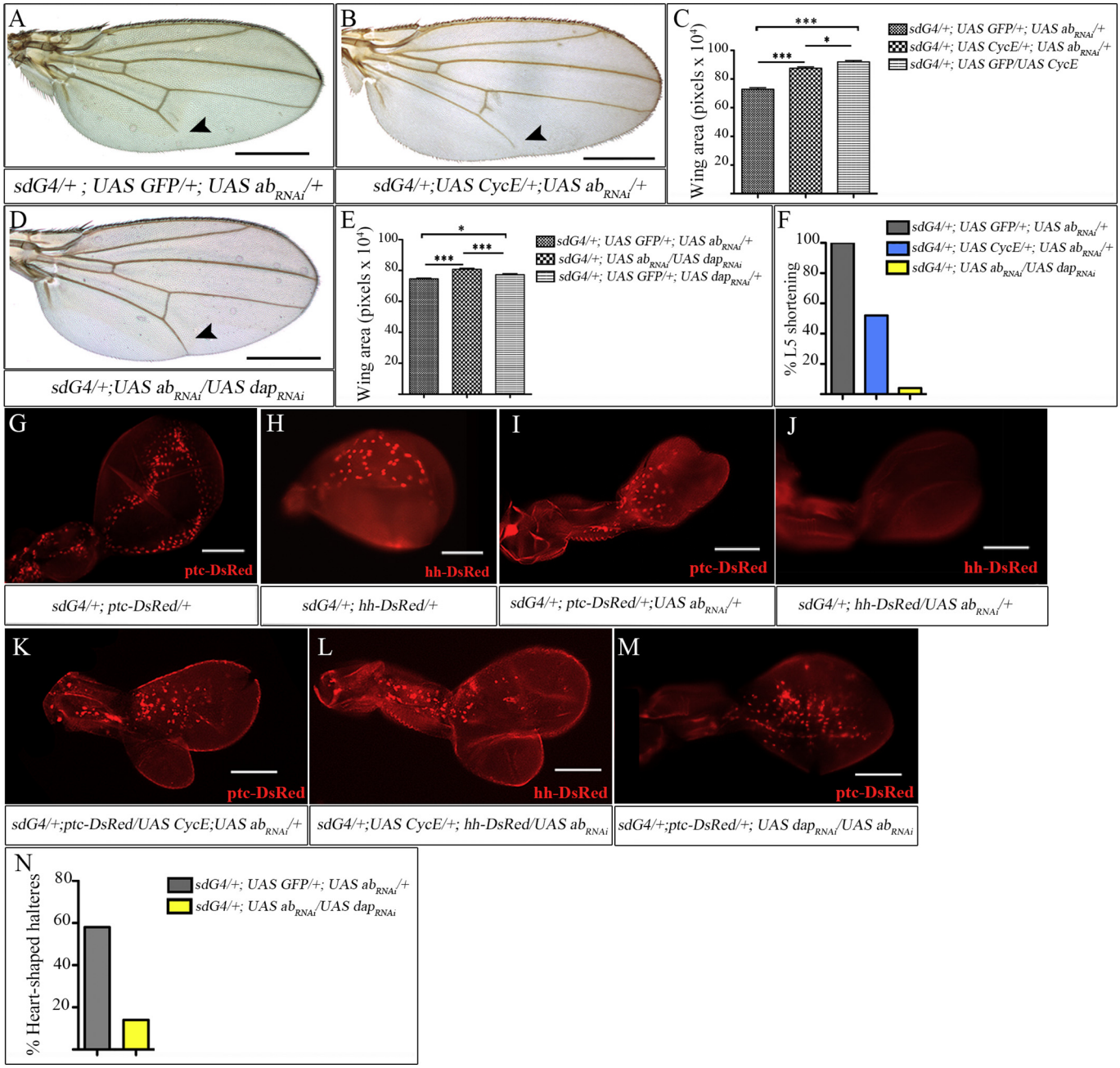

Fig. 6. *Cyclin E* and *dacapo* collaborate with *abrupt* to regulate wing and haltere size. A) Wing *sdG4/+; UAS GFP/+;UAS ab$_{RNAi}$/+*. Note the short L5 (arrowhead). B) *sdG4/+; UAS CycE/+; UAS ab$_{RNAi}$/+* wing. Note the rescue of the L5 length (arrowhead) and the rescue of the wing size. C) Graph representing wing area of the indicated genotypes (n = 20 of each genotype). Note that the size of the wing when *abrupt* is inactivated is modulated in the presence of high levels of *Cyclin E*. D) Wing *sdG4/+; UAS ab$_{RNAi}$/UAS dap$_{RNAi}$*. Note the rescue of the L5 length (arrowhead) compared to (A). E) Graph representing wing area of the indicated genotypes (n = 20 of each genotype). Note the size of the wing in conditions of *abrupt* inactivation is rescued when *dacapo* is also inactivated. F) Graph representing the percentage of wings showing short L5 vein of the indicated genotypes (n = 20 of each genotype). G) *sdG4/+; ptc-DsRed/+* haltere showing the expression pattern of *ptc-DsRed* (red) in the anterior compartment of the haltere. H) *sdG4/+; hh-DsRed/+* haltere showing the expression pattern of the *hh-DsRed* reporter (red) that marks the posterior compartment occupying about 30% of the haltere. I) *sdG4/+; ptc-DsRed/+; UAS ab$_{RNAi}$/+* haltere showing the expression of the *ptc-DsRed* (red) reporter. J) *sdG4/+; hh-DsRed/UAS ab$_{RNAi}$* haltere showing the expression pattern of the *hh-DsRed* reporter. K) Haltere *sdG4/+; ptc-DsRed/UAS CycE; UAS ab$_{RNAi}$/+* showing ptc-DsRed (red) expression. Compare with (G). L) Haltere *sdG4/+;UAS CycE/+; hh-DsRed/UAS ab$_{RNAi}$* showing hh-DsRed (red) expression. Compare with (H). M) Haltere *sdG4/+;ptc-DsRed/+;UAS ab$_{RNAi}$/UAS dap$_{RNAi}$* showing ptc-DsRed (red) expression. Compare with (I). N) Graph representing the percentage of heart-shaped halteres of the indicated genotypes (n = 90 for *sdG4/+; UAS GFP/+; UAS ab$_{RNAi}$/+* and n = 105 for *sdG4/+; UAS ab$_{RNAi}$/UAS dap$_{RNAi}$*). Scale bars represent 500 μm for wing and 50 μm for halteres. 0.01 < *p < 0.05, ***p < 0.001.

when overexpressed or when inactivated (Bejarano et al., 2012; Schertel et al., 2012; Szuplewski et al., 2012). However, the analysis of their mRNA targets in the control of growth has not been always clear. *miR-306* and *miR-275* share binding site sequences and the function of these miRNAs has been previously described to limit the expression of *bag of marbles* (*Bam*) in male germ line stem cells (Eun et al., 2013). The *abrupt* 3′-UTR contains a highly conserved seed match for *miR-306* (Fig. 5A, http://www.targetscan.org/fly) and it appears that the *abrupt* gene is targeted by multiple miRNAs (Bejarano et al., 2012; Okamura et al., 2008). Our work shows that *miR-306* regulates *abrupt* expression

(Fig. 5) and that both *miR-306* and *abrupt* interact to control wing size (Fig. 5J), thus defining a regulatory *miR-306/abrupt* axis. The overexpression of *miR-275* has also been found to eliminate the L5 vein of the wing (Bejarano et al., 2012). It would be interesting to determine if *miR-275* also contributes to the regulation of wing size through the regulation of *abrupt* expression.

Increased levels of Abrupt seem to influence the growth of the wing disc as overexpression of Abrupt leads to the development of tumor-like imaginal discs(Turkel et al., 2013; Simoes da Silva et al., 2017) (Fig. 4D–D″). It has been shown that high levels of Abrupt produce hyperplasia in the eye and wing imaginal discs, emphasizing the importance of microRNAs in the control of *abrupt* transcription levels to mediate *abrupt* oncogenic activity. RNA-seq expression profile analyses in conditions of Abrupt overexpression, have detected elevated levels of cell cycle regulators such as *cdk2*. Furthermore, ChIP-seq experiments indicate that the Abrupt protein binds to regulatory sequences of the *cdk2* gene (Turkel et al., 2013). *cdk2* is involved in the regulation of the G1-S transition together with the *Cyclin E*. Our results show that overexpression of Cyclin E and inactivation of *dacapo* rescue both the shortening of the L5 vein and the reduction of wing size that are associated with the inactivation of *abrupt* (Fig. 6B, D). Moreover, the size of the haltere is also rescued when Cyclin E is overexpressed (Fig. 6K–L) or when *dacapo* is inactivated (Fig. 6M–N).

Additionally, although the overexpression of Cyclin E rescues the decreased size of wing and haltere associated with the inactivation of *abrupt* (*sdG4/+; UAS Cyclin E/+;UAS* ab_{RNAi}/+) as well as the size of the haltere compartments, the “heart-shape” haltere phenotype is not rescued (compare Fig. 6I–J with K–L). It will be interesting to analyze the gene network involved in the generation of the indentation and the temporal window during which the indentation is formed to further understand the mechanisms through which *abrupt* controls growth. Furthermore, the results from our experiments do not allow us to distinguish whether Abrupt regulates directly or indirectly the expression of *Cyclin E* or *dacapo* indicating a collaborative function in the regulation of wing size or whether the observed rescue (Fig. 6) is a consequence of an additive effect when concomitantly increasing Cyclin E levels and lowering Abrupt levels. Moreover, the rescue observed could be due to the increase of proliferation, which is a consequence of forcing G1-S progression when manipulating Cyclin E and dacapo. However, further analyses are required to understand the functional relationship between these factors in the control of size of the appendages.

In conclusion, our results identify a novel role for *abrupt* in controlling the size of the wing and haltere and define a regulatory axis that involves the microRNA *miR-306*, the transcription factor Abrupt and cell cycle regulators. This regulatory axis may be of relevance to the control of the *abrupt* levels of transcription and therefore, the control of oncogenic activity associated with elevated Abrupt levels (Turkel et al., 2013) (Simoes da Silva et al., 2017). Interestingly, this function of *abrupt* in the control of size seems to be conserved in the beetle (Linz et al., 2016) and thus our results may serve to understand the evolutionarily function of *abrupt* in insects and mammals.

Supplementary data to this article can be found online at https://doi.org/10.1016/j.mod.2019.103555.

Acknowledgements

We thank Keith Harshman for carefully reading the manuscript, Stephen Crew for anti-Abrupt antibody, Olga Redondo for the initial characterization of the *miR-306-DsRed* lines and Ana Herrera and Milagros Pérez for technical assistance. We thank the Bloomington Stock Center for providing stocks and the Drosophila transgenic facility from the CBMSO for generation of transgenic flies. This work was supported by grants from Dirección general de investigación, Spain (BFU2008-01154, BFU2014-61881-EXP and BFU2017-83789-P) from Ministerio de Economía y Competitividad (MINECO), Spain and an Institutional grant to the CBMSO from Fundación Ramón Areces.

References

Akimoto, A., Wada, H., Hayashi, S., 2005. Enhancer trapping with a red fluorescent protein reporter in Drosophila. Dev. Dyn. 233, 993–997.
Becam, I., Rafel, N., Hong, X., Cohen, S.M., Milan, M., 2011. Notch-mediated repression of bantam miRNA contributes to boundary formation in the Drosophila wing. Development 138, 3781–3789.
Beira, J.V., Paro, R., 2016. The legacy of Drosophila imaginal discs. Chromosoma 125, 573–592.
Bejarano, F., Bortolamiol-Becet, D., Dai, Q., Sun, K., Saj, A., Chou, Y.T., Raleigh, D.R., Kim, K., Ni, J.Q., Duan, H., Yang, J.S., Fulga, T.A., Van Vactor, D., Perrimon, N., Lai, E.C., 2012. A genome-wide transgenic resource for conditional expression of Drosophila microRNAs. Development 139, 2821–2831.
Bender, W., Akam, M., Karch, F., Beachy, P.A., Peifer, M., Spierer, P., Lewis, E.B., Hogness, D.S., 1983. Molecular genetics of the bithorax complex in Drosophila melanogaster. Science 221, 23–29.
Brand, A.H., Perrimon, N., 1993. Targeted gene expression as a means of altering cell fates and generating dominant phenotypes. Development 118, 401–415.
Casanova, J., Sanchez-Herrero, E., Morata, G., 1985. Contrabithorax and the control of spatial expression of the bithorax complex genes of Drosophila. J. Embryol. Exp. Morphol. 90, 179–196.
Castelli-Gair, J., Greig, S., Micklem, G., Akam, M., 1994. Dissecting the temporal requirements for homeotic gene function. Development 120, 1983–1995.
Chen, Y.W., Song, S., Weng, R., Verma, P., Kugler, J.M., Buescher, M., Rouam, S., Cohen, S.M., 2014. Systematic study of Drosophila microRNA functions using a collection of targeted knockout mutations. Dev. Cell 31, 784–800.
Choo, S.W., White, R., Russell, S., 2011. Genome-wide analysis of the binding of the Hox protein Ultrabithorax and the Hox cofactor Homothorax in Drosophila. PLoS One 6, e14778.
Cook, O., Biehs, B., Bier, E., 2004. brinker and optomotor-blind act coordinately to initiate development of the L5 wing vein primordium in Drosophila. Development 131, 2113–2124.
Day, S.J., Lawrence, P.A., 2000. Measuring dimensions: the regulation of size and shape. Development 127, 2977–2987.
de Navas, L.F., Garaulet, D.L., Sanchez-Herrero, E., 2006. The ultrabithorax Hox gene of Drosophila controls haltere size by regulating the Dpp pathway. Development 133, 4495–4506.
de Nooij, J.C., Letendre, M.A., Hariharan, I.K., 1996. A cyclin-dependent kinase inhibitor, Dacapo, is necessary for timely exit from the cell cycle during Drosophila embryogenesis. Cell 87, 1237–1247.
Dichtel-Danjoy, M.L., Ma, D., Dourlen, P., Chatelain, G., Napoletano, F., Robin, M., Corbet, M., Levet, C., Hafsi, H., Hainaut, P., Ryoo, H.D., Bourdon, J.C., Mollereau, B., 2013. Drosophila p53 isoforms differentially regulate apoptosis and apoptosis-induced proliferation. Cell Death Differ. 20, 108–116.
Dietzl, G., Chen, D., Schnorrer, F., Su, K.C., Barinova, Y., Fellner, M., Gasser, B., Kinsey, K., Oppel, S., Scheiblauer, S., Couto, A., Marra, V., Keleman, K., Dickson, B.J., 2007. A genome-wide transgenic RNAi library for conditional gene inactivation in Drosophila. Nature 448, 151–156.
Eun, S.H., Stoiber, P.M., Wright, H.J., McMurdie, K.E., Choi, C.H., Gan, Q., Lim, C., Chen, X., 2013. MicroRNAs downregulate Bag of marbles to ensure proper terminal differentiation in the Drosophila male germline. Development 140, 23–30.
Ge, X., Zhang, Y., Jiang, J., Zhong, Y., Yang, X., Li, Z., Huang, Y., Tan, A., 2013. Identification of microRNAs in Helicoverpa armigera and Spodoptera litura based on deep sequencing and homology analysis. Int. J. Biol. Sci. 9, 1–15.
Gonzalez-Gaitan, M.A., Micol, J.L., Garcia-Bellido, A., 1990. Developmental genetic analysis of Contrabithorax mutations in Drosophila melanogaster. Genetics 126, 139–155.
Grubbs, N., Leach, M., Su, X., Petrisko, T., Rosario, J.B., Mahaffey, J.W., 2013. New components of Drosophila leg development identified through genome wide association studies. PLoS One 8, e60261.
Hammonds, A.S., Bristow, C.A., Fisher, W.W., Weiszmann, R., Wu, S., Hartenstein, V., Kellis, M., Yu, B., Frise, E., Celniker, S.E., 2013. Spatial expression of transcription factors in Drosophila embryonic organ development. Genome Biol. 14, R140.
Hattori, Y., Usui, T., Satoh, D., Moriyama, S., Shimono, K., Itoh, T., Shirahige, K., Uemura, T., 2013. Sensory-neuron subtype-specific transcriptional programs controlling dendrite morphogenesis: genome-wide analysis of Abrupt and Knot/Collier. Dev. Cell 27, 530–544.
Hay, B.A., Wassarman, D.A., Rubin, G.M., 1995. Drosophila homologs of baculovirus inhibitor of apoptosis proteins function to block cell death. Cell 83, 1253–1262.
Herranz, H., Hong, X., Perez, L., Ferreira, A., Olivieri, D., Cohen, S.M., Milan, M., 2010. The miRNA machinery targets Mei-P26 and regulates Myc protein levels in the Drosophila wing. EMBO J. 29, 1688–1698.
Hu, S., Fambrough, D., Atashi, J.R., Goodman, C.S., Crews, S.T., 1995. The Drosophila abrupt gene encodes a BTB-zinc finger regulatory protein that controls the specificity of neuromuscular connections. Genes Dev. 9, 2936–2948.
Jagadeeswaran, G., Zheng, Y., Sumathipala, N., Jiang, H., Arrese, E.L., Soulages, J.L., Zhang, W., Sunkar, R., 2010. Deep sequencing of small RNA libraries reveals dynamic regulation of conserved and novel microRNAs and microRNA-stars during silkworm development. BMC Genomics 11, 52.
Jang, A.C., Chang, Y.C., Bai, J., Montell, D., 2009. Border-cell migration requires integration of spatial and temporal signals by the BTB protein Abrupt. Nat. Cell Biol. 11, 569–579.
Johnston, L.A., Gallant, P., 2002. Control of growth and organ size in Drosophila.

Bioessays 24, 54–64.
Kauffman, S.A., 1981. Patterns of temperature sensitivity in Contrabithorax/Ultrabithorax heterozygotes of Drosophila. Dev. Biol. 88, 341–351.
Lander, A.D., 2011. Pattern, growth, and control. Cell 144, 955–969.
Lane, M.E., Sauer, K., Wallace, K., Jan, Y.N., Lehner, C.F., Vaessin, H., 1996. Dacapo, a cyclin-dependent kinase inhibitor, stops cell proliferation during Drosophila development. Cell 87, 1225–1235.
Lewis, J., 2008. From signals to patterns: space, time, and mathematics in developmental biology. Science 322, 399–403.
Li, W., Wang, F., Menut, L., Gao, F.B., 2004. BTB/POZ-zinc finger protein abrupt suppresses dendritic branching in a neuronal subtype-specific and dosage-dependent manner. Neuron 43, 823–834.
Linz, D.M., Hu, A.W., Sitvarin, M.I., Tomoyasu, Y., 2016. Functional value of elytra under various stresses in the red flour beetle, Tribolium castaneum. Sci. Rep. 6, 34813.
Macedo, L.M., Nunes, F.M., Freitas, F.C., Pires, C.V., Tanaka, E.D., Martins, J.R., Piulachs, M.D., Cristino, A.S., Pinheiro, D.G., Simoes, Z.L., 2016. MicroRNA signatures characterizing caste-independent ovarian activity in queen and worker honeybees (Apis mellifera L.). Insect Mol. Biol. 25, 216–226.
Mirth, C.K., Shingleton, A.W., 2012. Integrating body and organ size in Drosophila: recent advances and outstanding problems. Front. Endocrinol. (Lausanne) 3, 49.
Morgan, T.H., Bridges, C.B., Sturtevant, A.H., 1925. The Genetics of *Drosophila melanogaster*.
Neto-Silva, R.M., Wells, B.S., Johnston, L.A., 2009. Mechanisms of growth and homeostasis in the Drosophila wing. Annu. Rev. Cell Dev. Biol. 25, 197–220.
Okamura, K., Phillips, M.D., Tyler, D.M., Duan, H., Chou, Y.T., Lai, E.C., 2008. The regulatory activity of microRNA* species has substantial influence on microRNA and 3′ UTR evolution. Nat. Struct. Mol. Biol. 15, 354–363.
Pan, D., 2010. The hippo signaling pathway in development and cancer. Dev. Cell 19, 491–505.
Pavlopoulos, A., Akam, M., 2011. Hox gene Ultrabithorax regulates distinct sets of target genes at successive stages of Drosophila haltere morphogenesis. Proc. Natl. Acad. Sci. U. S. A. 108, 2855–2860.
Restrepo, S., Zartman, J.J., Basler, K., 2014. Coordination of patterning and growth by the morphogen DPP. Curr. Biol. 24, R245–R255.
Richardson, H., O'Keefe, L.V., Marty, T., Saint, R., 1995. Ectopic cyclin E expression induces premature entry into S phase and disrupts pattern formation in the Drosophila eye imaginal disc. Development 121, 3371–3379.
Robertson, F.W., 1959. Studies in quantitative inheritance. XII. Cell size and number in relation to genetic and environmental variation of body size in Drosophila. Genetics 44, 869–896.
Roch, F., Akam, M., 2000. Ultrabithorax and the control of cell morphology in Drosophila halteres. Development 127, 97–107.
Schertel, C., Rutishauser, T., Forstemann, K., Basler, K., 2012. Functional characterization of Drosophila microRNAs by a novel in vivo library. Genetics 192, 1543–1552.
Simoes da Silva, C.J., Fereres, S., Simon, R., Busturia, A., 2017. Drosophila SCE/dRING E3-ligase inhibits apoptosis in a Dp53 dependent manner. Dev. Biol. 429, 81–91.
Simon, E., Guerrero, I., 2015. The transcription factor optomotor-blind antagonizes Drosophila haltere growth by repressing decapentaplegic and hedgehog targets. PLoS One 10, e0121239.
Smolik-Utlaut, S.M., 1990. Dosage requirements of Ultrabithorax and bithoraxoid in the determination of segment identity in Drosophila melanogaster. Genetics 124, 357–366.
Sugimura, K., Satoh, D., Estes, P., Crews, S., Uemura, T., 2004. Development of morphological diversity of dendrites in Drosophila by the BTB-zinc finger protein abrupt. Neuron 43, 809–822.
Szuplewski, S., Kugler, J.M., Lim, S.F., Verma, P., Chen, Y.W., Cohen, S.M., 2012. MicroRNA transgene overexpression complements deficiency-based modifier screens in Drosophila. Genetics 190, 617–626.
Teleman, A.A., Cohen, S.M., 2000. Dpp gradient formation in the Drosophila wing imaginal disc. Cell 103, 971–980.
Turkel, N., Sahota, V.K., Bolden, J.E., Goulding, K.R., Doggett, K., Willoughby, L.F., Blanco, E., Martin-Blanco, E., Corominas, M., Ellul, J., Aigaki, T., Richardson, H.E., Brumby, A.M., 2013. The BTB-zinc finger transcription factor abrupt acts as an epithelial oncogene in Drosophila melanogaster through maintaining a progenitor-like cell state. PLoS Genet. 9, e1003627.
Vactor, D.V., Sink, H., Fambrough, D., Tsoo, R., Goodman, C.S., 1993. Genes that control neuromuscular specificity in Drosophila. Cell 73, 1137–1153.
Vollmer, J., Casares, F., Iber, D., 2017. Growth and size control during development. Open Biol. 7.
Waldron, J.A., Newbury, S.F., 2012. The roles of miRNAs in wing imaginal disc development in Drosophila. Biochem. Soc. Trans. 40, 891–895.
Weatherbee, S.D., Halder, G., Kim, J., Hudson, A., Carroll, S., 1998. Ultrabithorax regulates genes at several levels of the wing-patterning hierarchy to shape the development of the Drosophila haltere. Genes Dev. 12, 1474–1482.
Ylla, G., Fromm, B., Piulachs, M.D., Belles, X., 2016. The microRNA toolkit of insects. Sci. Rep. 6, 37736.